PERGAMON

Phytochemistry 61 (2002) 7–14

PHYTOCHEMISTRY

www.elsevier.com/locate/phytochem

Structure of cellulose-deficient secondary cell walls from the *irx3* mutant of *Arabidopsis thaliana*

Marie-Ann Ha[a], Iain M. MacKinnon[a], Adriana Šturcová[a], David C. Apperley[b], Maureen C. McCann[c], Simon R. Turner[d], Michael C. Jarvis[a,*]

[a]*Chemistry Department, Glasgow University, Glasgow G12 8QQ, Scotland, UK*
[b]*EPSRC Solid-state NMR Service, Durham University, Durham DH1 3LE, UK*
[c]*Department of Cell and Developmental Biology, John Innes Research Institute, Norwich NR4 7UH, UK*
[d]*School of Biological Science, University of Manchester, Manchester M13 9PT, UK*

Received 17 April 2002; received in revised form 28 May 2002

Abstract

In the *Arabidopsis* mutant *irx3*, truncation of the *AtCesA7* gene encoding a xylem-specific cellulose synthase results in reduced cellulose synthesis in the affected xylem cells and collapse of mature xylem vessels. Here we describe spectroscopic experiments to determine whether any cellulose, normal or abnormal, remained in the walls of these cells and whether there were consequent effects on other cell-wall polysaccharides. Xylem cell walls from *irx3* and its wild-type were prepared by anatomically specific isolation and were examined by solid-state NMR spectroscopy and FTIR microscopy. The affected cell walls of *irx3* contained low levels of crystalline cellulose, probably associated with primary cell walls. There was no evidence that crystalline cellulose was replaced by less ordered glucans. From the molecular mobility of xylans and lignin it was deduced that these non-cellulosic polymers were cross-linked together in both *irx3* and the wild-type. The disorder previously observed in the spatial pattern of non-cellulosic polymer deposition in the secondary walls of *irx3* xylem could not be explained by any alteration in the structure or cross-linking of these polymers and may be attributed directly to the absence of cellulose microfibrils which, in the wild-type, scaffold the organisation of the other polymers into a coherent secondary cell wall.

Keywords: *Arabidopsis*; Cruciferae; Cellulose; Cell walls; Cellulose synthases; Lignin; Mobility; Solid-state NMR

1. Introduction

Cellulose in higher plants is synthesised at the plasma membrane by a multi-enzyme complex comprising multiple catalytic subunits and other proteins (Delmer, 1999). The *CesA* gene family, with sequence similarity to genes encoding the catalytic polypeptide of bacterial cellulose synthase, probably has about 30 members in *Arabidopsis* (Taylor et al., 2000). Some of these may encode other polysaccharide synthases but about one-third of the *Arabidopsis CesA* genes for which sequence and functional evidence is available form a homologous group, within which evidence of involvement in cellulose synthesis is strong (Pear et al., 1996; Arioli et al., 1998; Taylor et al., 1999; Fagard et al., 2000a,b).

It seems reasonable that products of different *CesA* genes involved in cellulose synthesis are targeted to different cell types, with different types of cell wall (Fagard et al., 2000b). It has also been suggested that the synthesis of each microfibril requires the concerted action of two or more *CesA* gene products (Taylor et al., 2000). A number of *Arabidopsis* mutants at *CesA* loci have phenotypes that support these suppositions. They include *rsw1* (Arioli et al., 1998) with a mutation in *AtCesA1*, and *procuste* (Fagard et al., 2000a) with a mutation in *AtCesA6,* both of which appear to affect primary cell walls in rapidly elongating tissues. In *irx3*, a mutant in *AtCesA7,* cellulose synthesis is defective in the thickened secondary cell walls of xylem and interfascicular tissues in the stem (Turner and Somerville, 1997). In the collapsed xylem phenotype which results, the walls of

* Corresponding author. Tel.: +44-141-330-4653; fax: +44-141-330-4888.
E-mail address: mikej@chem.gla.ac.uk (M.C. Jarvis).

0031-9422/02/$ - see front matter
PII: S0031-9422(02)00199-1

xylem vessels lose cohesion and, in mature plants, collapse inwards under hydrostatic pressure (Turner and Somerville, 1997). The cellulose content of mature *irx3* stems is some 30% of that of the wild-type (Turner and Somerville, 1997; Taylor et al., 1999) when determined by the Updegraff method (Updegraff, 1969). This may of course include cellulose present in other tissues not affected by the *irx3* mutation. It is therefore not certain whether cellulose is absent from the affected cell walls nor whether, if any cellulose is present, it is normal or altered in structure or supramolecular assembly.

Arioli et al. (1998) suggested that *rsw1* accumulates atypical soluble glucans whose relationship to crystalline cellulose is not clear. They hypothesised that in *rsw1* the catalytic subunit is functional but is not integrated into the synthetic complex in such a way as to permit normal assembly of the synthetic 'rosette' complexes or hence the assembly of normal microfibrils (Arioli et al., 1998). There is also evidence for release of relatively soluble glucan-containing fractions when the rosettes are disrupted by herbicide action (Peng et al., 2001). Recent studies (Nicol et al., 1998; Lane et al., 2001; Sato et al., 2001) have identified a putative endoglucanase that is required for cellulose synthesis and is deficient in *kor* plants, which also contain a soluble glucan (Lane et al., 2001). Soluble glucans would presumably not be determined as cellulose by the Updegraff procedure, which requires a degree of crystallinity to provide resistance to acid hydrolysis, and they might therefore be absent or present in *irx3* on existing evidence (Turner and Somerville, 1997). Taken together these results invite the question whether or not a soluble glucan is present in all cellulose deficient plants, and how it might be synthesised.

In the study of the *irx3* phenotype by Turner and Somerville (1997) xylan and lignin as well as cellulose contents were measured in whole mature stems. Since the visible phenotype was restricted to xylem and interfascicular tissues these measurements must have underestimated the extent of differences from the wild-type, to a degree that is uncertain. In a number of systems where cellulose synthesis in primary cell walls is impaired by mutation (Peng et al., 2000; Fagard et al., 2000a; His et al., 2001) or by herbicide action (Shedletzky et al., 1990), a less branched, more acidic pectin matrix is produced. This may assume part of the load-bearing function of the missing cellulose. It is not clear if there are any similar, compensatory alterations in the non-cellulosic polymers of the cellulose-depleted secondary cell walls in *irx3*. Lignin levels measured by Turner and Somerville (1997) were similar to the wild-type stems but electron-dense material, apparently lignin, was visible by TEM as diffuse deposits in the lumina of collapsed xylem vessels (Taylor et al., 1992). This raises several questions. Are the non-cellulosic polymers of *irx3* altered in structure or only in the spatial pattern of their deposition? Does the deposition pattern result merely from absence of the spatial order imposed on wild-type wall architecture by cellulose? Would any structural alterations restore limited mechanical strength to cellulose-deficient cell walls?

Previous experiments on *irx3* and other cellulose mutants have involved either chemical studies on whole plant organs or classical histology. To focus on the wall structure of the cells that express the *irx3* mutation, and only these cells, we adopted two new approaches. Firstly we isolated cell walls specifically from the vascular ring of inflorescence stems of *irx3*. We examined these cell walls in solid state NMR experiments that are sensitive to the crystalline form of any cellulose present, and to the molecular rigidity of the non-cellulosic matrix. Secondly we examined the distribution and structure of crystalline cellulose in specific tissues of inflorescence stems by FTIR-microspectroscopy of deuterated thin sections.

2. Results

2.1. Cell-wall isolation

Controlled mechanical disintegration followed by differential sieving is an established method for isolating anatomically specific cell-wall preparations from brassica stems (Wilson et al., 1988). This technique was applied to mature *Arabidopsis* stems after removal of the epidermis by freezing and peeling. The resulting cell walls were derived from the xylem and interfascicular tissues with a high degree of specificity, although they were not anatomically homogeneous as these tissues contain a number of cell types. The compositional data (Table 1) showed that cellulose as measured by the Updegraff (1969) method was severely depleted in these cell wall preparations from *irx3* and that the non-cellulosic polysaccharides were principally xylose polymers as is typical in sclerenchymatous tissues.

Table 1
Carbohydrate composition of wild-type and *irx3* sclerenchyma cell walls

	Wild-type		*irx3*	
	Mean	S.E.M.	Mean	S.E.M.
Non-cellulosic sugars, % of total recovered after acid hydrolysis				
Fucose	3.1	0.1	2.8	0.4
Arabinose	3.9	0.1	4.9	0.7
Xylose	69.0	0.6	73.9	3.3
Mannose	7.4	0.3	5.1	0.7
Galactose	5.3	0.1	6.0	0.5
Glucose	11.3	0.1	7.2	0.5
Cellulose, as % acid-insoluble glucose in cell wall				
	30.95	4.15	6.11	0.64

2.2. Solid-state NMR spectroscopy

The solid-state ^{13}C NMR spectra of the sclerenchyma cell walls differed greatly between *irx3* and the wild-type (Fig. 1A and B). A ^{13}C spectrum of the material present in the wild-type but lacking in *irx3* was derived by taking linear combinations of the *irx3* and wild-type spectra (Fig. 1C), and showed that this material had the spectral characteristics of essentially pure cellulose. Expansion of the C-4 spectral region (Fig. 1, inset) made it clear that crystal-interior cellulose Iα and Iβ and the surface form of cellulose (Ha et al., 1998) were all depleted in *irx3*. The proportion of surface to interior chains in the cellulose missing from *irx3* (Fig. 1C) indicates crystalline units with about 20 chains, typical of woody dicotyledonous cell walls (Newman, 1998). The amount of cellulose detectable in the *irx3* sclerenchyma cell walls was consistent with the chemical data in Table 1 but was too small for structural characterisation by ^{13}C NMR, since the distinctive surface C-4 peaks were overlapped by the much larger C-4 peak from β(1,4)-linked xylan chains.

A different set of linear combinations of the *irx3* and wild-type solid-state ^{13}C NMR spectra (Fig. 1D) gave a composite spectrum derived from those polymer components that were more abundant in the *irx3* cell walls. The composite spectrum was consistent with the presence of more acetylated glucuronoarabinoxylan and lignin in the *irx3* cell walls, but because the study was carried out on isolated cell walls this could in principle represent either an absolute increase in the abundance of these polymers or a relative enrichment due to the absence of cellulose. The data of Turner and Somerville (1997) imply a relative, not an absolute, increase in the abundance of arabinoxylan. On that assumption the cellulose content of the cell walls was reduced by just over 70% as calculated from the coefficients used in the linear combinations of the spectra. This is comparable with the (80±4%) reduction in Updegraff cellulose (Table 1).

Based on the intensity of the methoxyl signal at 56 ppm, the lignin content of the cell walls was estimated as 200 mg/g in the wild-type and 305 mg/g in *irx3*. These figures are equivalent respectively to 29% and 32% of the non-cellulosic fraction of the cell walls, suggesting that the difference in cell-wall lignin content was merely relative and ensued from lack of cellulose in *irx3*. It is more common and normally more accurate to calculate lignin content from the total signal from quaternary ^{13}C nuclei. In this case the short contact time required for the relaxation experiments was inappropriate for quantitative estimation of quaternary carbon atoms, so that low estimates of the lignin content were obtained, although still with little difference between *irx3* and the wild-type when expressed relative to the non-cellulosic fraction of the cell walls (data not shown). The calculation from methoxyl data is approximate due to the variable methoxyl content of lignins, which depends on the guaiacyl/syringyl (G/S) ratio. However, the relative intensity of the signal at 153 ppm from C-3 and C-5 of S residues was similar in the spectra from *irx3* and the wild-type, indicating that their lignins did not differ greatly in G/S ratio. There was no indication of any other abnormality in composition in the lignin spectrum in *irx3* cell walls, which was similar to the wild-type and qualitatively typical of dicot lignin spectra.

2.3. NMR relaxation experiments

The relaxation of nuclear magnetism in solids is influenced by thermal motion and can be used to probe molecular mobility in the different components of a composite material such as a plant cell wall (Newman et al., 1996; Ha et al., 1997). Here we used proton spin relaxation editing (PSRE; Ha et al., 1997) to obtain the NMR spectra (subspectra) characteristic of the mobile and rigid material in the sclerenchyma cell walls of wild-type *Arabidopsis* stems. The procedure is based on interpolymer differences in the proton rotating-frame spin-lattice relaxation time $T_{1\rho}$, which is sensitive to thermal motion on the kHz frequency scale. Cellulose is normally the most rigid polymer in plant cell walls (Newman et al., 1996; Ha et al., 1997) but the rigidity of lignin can also be considerable (Newman, 1998). The 'mobile' and 'rigid' subspectra of the wild type cell walls are shown in Fig. 1E and F. All polymer components represented in the ^{13}C spectrum of *irx3* cell walls were similar in proton $T_{1\rho}$ so that no separation into 'mobile' and 'rigid' subspectra was possible. However, the peak positions and the relative intensities in the entire spectrum of *irx3* were in agreement with the peak positions and the relative intensities in the 'mobile' subspectrum of the wild-type cell walls (Table 2; compare Fig. 1B with Fig. 1F).

2.4. FTIR microscopy

By deuterating cellulose with D_2O in the vapour phase it is possible to convert the hydroxyl groups of the surface chains of cellulose and other accessible polymers to –OD, leaving only the interior chains of cellulose in the hydroxyl form (Tsuboi, 1957). Since the –OH and –OD stretching vibrational modes are sensitive to hydrogen bonding and are readily observable by FTIR microscopy, this potentially allows the characteristic hydrogen-bonding pattern of the cellulose interior chains to be observed at the single-cell level. FTIR microspectra of deuterated fibres and tracheary elements in the secondary xylem of *irx3* are compared to its wild-type in Fig. 2. To obtain adequate freedom from scattering effects the aperture area used corresponded to that of 2–5 cells. These are not single-cell

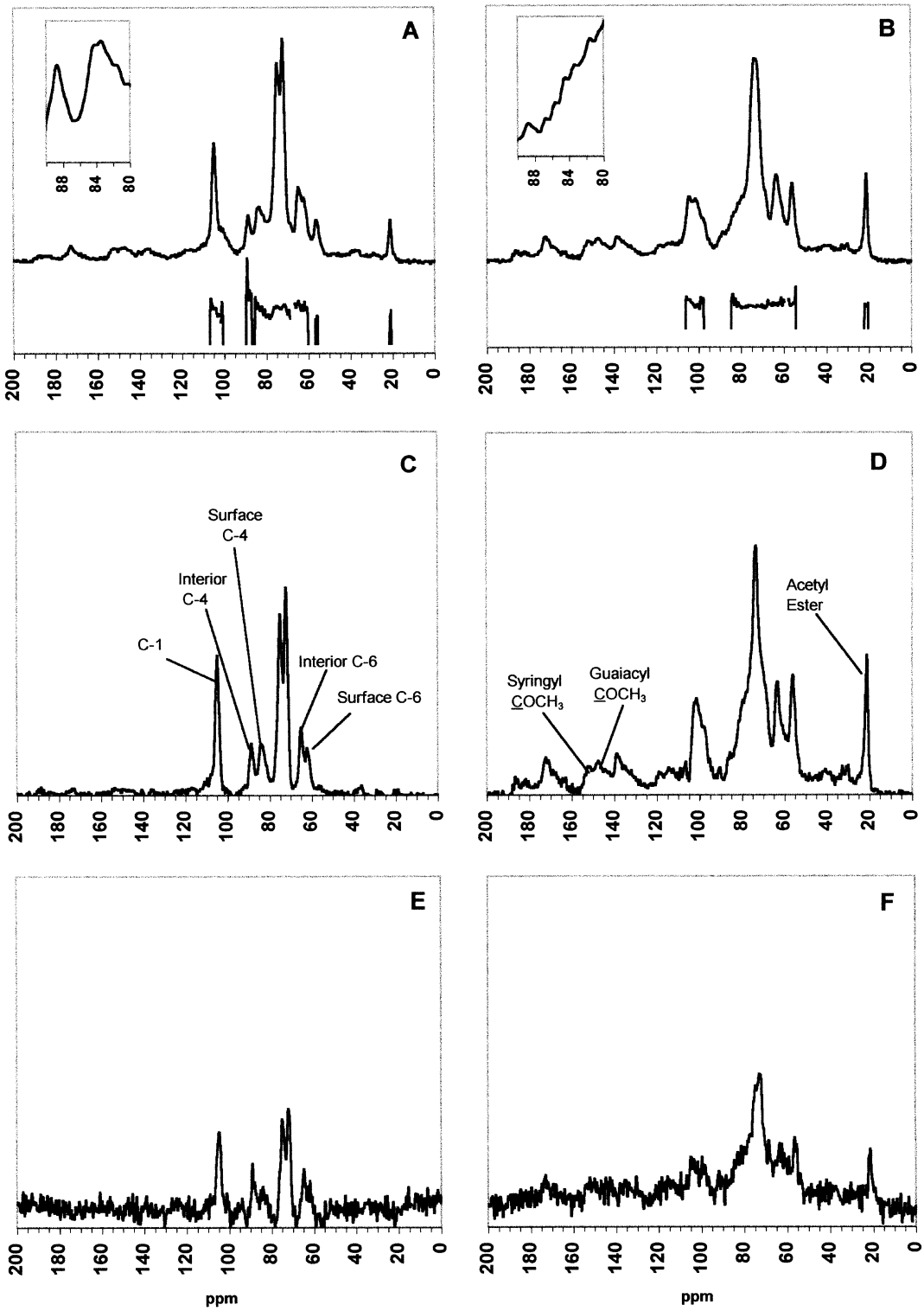

Fig. 1. Solid-state ^{13}C NMR spectra of the secondary xylem cell walls of the wild-type (A) and *irx3* (B) with proton rotating frame spin-lattice relaxation time (^{1}H $T_{1\rho}$) shown below the spectra. Rapid relaxation (short ^{1}H $T_{1\rho}$) indicates high molecular mobility. Gaps in the plot of $T_{1\rho}$ correspond to spectral regions with insufficient signal to determine this relaxation time constant. The maximum value of the ^{1}H $T_{1\rho}$ at 90 ppm in A is an artefact caused by slightly greater line-broadening in the spectrum with the delayed-contact pulse. The inset of A shows in more detail the 84–89 ppm region of the wild type spectrum with peaks diagnostic of the interior and surface cellulosic C-4. C shows the essentially cellulosic spectrum derived by subtracting the *irx3* spectrum from the wild type. Conversely D, the spectrum obtained by subtracting the wild type spectrum from *irx3*, is typical of dicot lignin plus glucuronoarabinoxylan. E and F show subspectra derived from ^{13}C NMR spectrum of wild type (A) by proton spin relaxation editing. The spectrum of the less mobile polymers in the wild type of *Arabidopsis* (the 'rigid' subspectrum) corresponds to the solid microfibril phase of cellulose chains (E). The 'mobile' subspectrum represents the xylan and lignin networks (F).

Table 2
Signal assignments and intensities in ^{13}C NMR spectra of sclerenchyma cell walls of the wild type (the 'mobile' subspectrum from PSRE: see Fig. 1F and Experimental) and the *irx3* mutant of *Arabidopsis* (Fig. 1B)

Polymer	Carbon	Chemical shift in wild type (ppm)	Chemical shift in *irx3* (ppm)	Relative intensity—wild type (%)	Relative intensity—*irx3* (%)
Cellulose[a]	C-1	103.6	104.1	25	28
Xylan	C-1	98.2	100.8	18	26
All glycans		72.3	72.9	100	100
Xylan	C-5	62.6	63.5	39	40
Lignin[b]	O$\underline{C}H_3$	56.5	56.1	43	35
Acetyl	$\underline{C}H_3$–	21.3	21.3	34	41

Relative intensity values are calculated as a percentage of the intensity of the 72.3 ppm peak which contains contributions from all polysaccharides.

[a] The cellulose C-1 signal is normally at 105 ppm but is displaced upfield, in these spectra, by overlap with the more intense and very broad xylan C-1 signal.

[b] Aromatic carbon signals from lignin in the 120–160 ppm spectral range are also present (assigned in Fig. 1D) but are less suitable for quantification of lignin than the O$\underline{C}H_3$ peak because their cross-polarisation kinetics differ greatly from the carbohydrate signals.

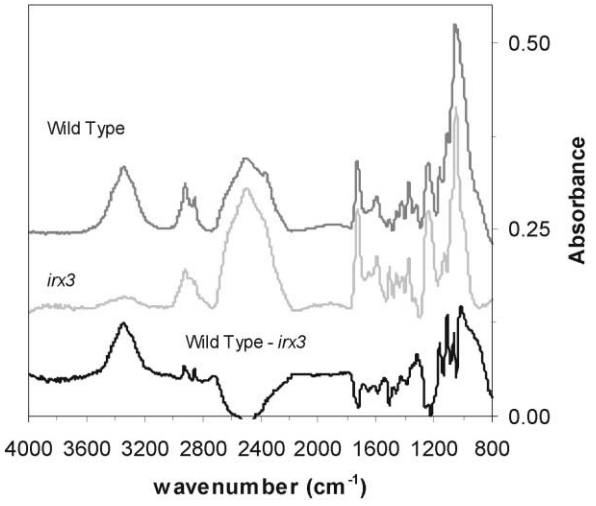

Fig. 2. FTIR spectra of sclerenchyma tissues from mature hypocotyls of wild type and *irx3* after vapour phase deuterium exchange. The low intensity of the residual OH stretching band in the *irx3* spectrum indicates severely depleted crystalline cellulose within its cell walls. Subtraction of the two spectra prior to baseline correction demonstrates that the 1165 and 1105 cm^{-1} peaks, indicative of cellulosic material, are also diminished in the *irx3* spectrum relative to the wild type.

spectra, therefore, but the spatial resolution is sufficient to distinguish the different cell types within the xylem and interfascicular regions.

Deuteration removed most of the hydroxyl stretching intensity to the 2500 cm^{-1} region typical of OD groups, revealing OH stretching bands from crystalline interior chains of cellulose Iα and Iβ (Sugiyama et al., 1991) in the wild-type (Fig. 2). In *irx3* these were severely depleted. The residual level was 16% of the wild-type level with a standard deviation of 7%. The anomeric stretching band at 1165 cm^{-1}, specific for cellulose chains in whatever form (Sugiyama et al., 1991), was likewise greatly diminished in *irx3* tissue sections compared with the wild-type. The mean shape of the residual hydroxyl stretching bands in *irx3*, although not identical with those of the wild-type, was within the normal range for crystalline cellulose in *Arabidopsis* tissues (Jarvis and McCann, 2000 and unpublished data).

3. Discussion

3.1. Residual cellulose in irx3 sclerenchyma cell walls

Isolating sclerenchyma cell walls allowed us to assess the effects of the *irx3* mutation on the tissues where the collapsed xylem phenotype is expressed. Our results confirm the ultrastructural observations of Turner and Somerville (1997) that cellulose synthesis in the cell walls of the xylem and interfascicular tissues is severely disrupted by the mutation to *AtCesA7*. Little cellulose remained in the sclerenchyma cell-wall preparations from *irx3*.

The cellulose content of these cell-wall preparations was not zero, however, and it would be useful to know whether or not the residual cellulose was located in the secondary cell-wall layers themselves. Some of the residual cellulose detected by NMR is likely to have been present in non-lignified walls of xylem parenchyma cells. However, the spatial resolution available by FTIR microscopy avoids any such problems of anatomical heterogeneity. A small amount of residual cellulose was still consistently detected in the FTIR spectra from fibres and tracheids in *irx3*. These spectra also contained bands characteristic of both pectin (1740, 1250 cm^{-1}) and lignin (1510 cm^{-1}), implying that the cells concerned had both primary and secondary wall layers. It has been noted (e.g. Wilson et al., 1988; Engels and Jung, 1998) that tracheary elements and especially fibre cells in herbaceous stems retain their primary walls after secondary wall formation is complete, whereas in mature wood the primary walls are degraded. It is thus likely that the residual cellulose detected was of primary-wall origin. The presence of primary walls in the sclerenchyma cell-wall preparations is also evident from the NMR spectra of *irx3*, where a distinctive shoulder at 69 ppm is characteristic of pectins (Ha et al., 1997).

The data presented are consistent with the hypothesis that cellulose synthesis was completely blocked in the secondary wall layers of xylem and interfascicular cells of *irx3*. Due to the presence of primary-wall layers in the wall examined we cannot exclude the alternative possibility that a few percent of the wild-type cellulose level remained in the secondary wall layers, but the reduced cellulose content in the *irx3* cell-wall preparations

is much more striking than was apparent from the previous analysis of entire stems (Turner and Somerville, 1997).

The deuteration-resistant (crystalline) cellulose remaining in the affected *irx3* tissues appeared to be structurally normal from the FTIR microspectra. There was no evidence for the presence of aberrant non-crystalline forms of cellulose as reported by Arioli et al. (1998) either as elevated levels of glucose in the acid-hydrolysable fraction or as a more mobile component in the ^{13}C NMR spectra. Published reports on the amorphous glucan state that oxalate extraction is required to extract it from cell walls (Arioli et al., 1998; Peng et al., 2000; Lane et al., 2001). It is unlikely, therefore, that such material would be lost during our cell wall isolation procedure. We infer that although crystalline cellulose is severely depleted in the affected tissues of *irx3*, if any soluble glucan is formed in its place the quantity is minimal, within the limits of error of the non-cellulosic glucose analysis.

This raises intriguing questions about how the soluble glucan arises in other cellulose deficient mutants such as *rsw1* and *kor1*. Null *kor* alleles are lethal (Zuo et al., 2000). Consequently soluble glucan has only been detected in relatively weak alleles of kor. Similarly the temperature sensitive *rsw1* mutant is a relatively weak allele. In constrast since no protein can be detected in the mutant plants, *irx3* plants are completely null alleles (Taylor et al., 2000). The apparent absence of soluble glucan in *irx3* plants suggests that the partially functional protein in weak alleles of *rsw1* or *kor* plants might contribute to the synthesis of this polymer. An alternative explanation relates to the fact that both *rsw1* and *kor* affect primary cell walls and the soluble glucan might be synthesised in response to the decreased strength of the wall in a manner similar to the increase in pectin (see below).

3.2. Non-cellulosic polymers

To our knowledge this is the first time that the polysaccharide composition of intact secondary cell walls of *Arabidopsis* has been studied spectroscopically. Their solid-state ^{13}C NMR spectra were quite similar to those of angiosperm wood (Newman, 1998).

From the PSRE experiment based on ^{1}H $T_{1\rho}$ values, which decrease with polymer mobility on the kHz frequency scale, cellulose was the most rigid polymer present in the wild-type cell walls. The xylan and lignin components were more mobile than cellulose and, as in *irx3,* had similar ^{1}H $T_{1\rho}$ values to one another. This corresponds to observations on angiosperm wood (Newman and Hemmingson, 1990) and could arise either because the cross-linked, relatively rigid lignin macromolecule was bonded to the xylans by ester and ether linkages (Helm, 2000), conferring similar rigidity on the xylans; or because the two macromolecules were intimately enough mixed for their $T_{1\rho}$ values to be averaged by ^{1}H spin diffusion. The first explanation is more likely because the xylans are expected to be in close proximity also to cellulose in the wild-type cell walls, but the ^{1}H $T_{1\rho}$ values of these two polysaccharides were distinct. We infer that in both *irx3* and its wild-type the xylans were stiffened at the molecular level by lignin bonded to them, but that this did not prevent the spatial disorganisation of both non-cellulosic polymers during their deposition in *irx3*. There was no sign of any structural changes to the lignin–glucuronoarabinoxylan complex in *irx3* that might increase its rigidity over that in the wild-type to compensate for the absence of cellulose, in a manner analogous to pectins in cellulose-deficient primary walls (His et al., 2001).

Without covalent cross-linking by lignin the xylan component would presumably be water-soluble. Assuming that the diffuse, electron dense deposits observed in collapsed xylem vessels of *irx3* by Turner and Somerville (1997) contained both xylan and lignin, our results imply that covalent bonding between them provides insolubility but is not enough to create a mechanically coherent secondary cell wall in the absence of cellulose. Instead it would appear that cellulose microfibrils are needed to organise the non-cellulosic polymers into the characteristic spatial pattern of the secondary wall thickenings, and that this does not happen in *irx3*. Cellulose is therefore required in the vessel cell walls to provide the architectural organisation and the radial compressive strength to withstand the negative pressures involved in a fully functional water transport system.

4. Experimental

4.1. Plant materials

Plants were grown at 22 °C in continuous light at light intensity of 120–150 μE m^{-2}. Stem material was harvested from inflorescences 10–20 cm tall, frozen in liquid nitrogen and freeze dried overnight.

4.2. Isolation of sclerenchyma cell walls

Freeze-dried *Arabidopsis* stems were rehydrated, frozen and thawed. Epidermal and cortical tissues were removed using a scalpel blade. The residual stem material was homogenised (6×15 s) in a Waring blender in 2% Triton X100, and wet-sieved through stacked stainless steel square-mesh sieves to separate primary and secondarily thickened cell walls (Wilson et al., 1988). Sclerenchyma cell walls were collected on a 850-μm sieve and primary cell walls on a 150-μm sieve. All aqueous solutions used during cell wall isolation contained mixed

cation-buffer (10 mM NaOAc, 3 mM KCl, 2 mM $MgCl_2$ and 1 mM $CaCl_2$, pH 6.5) designed to mimic the ionic conditions of the apoplast (Goldberg et al., 1996). Tissues were stirred in 80% phenol to remove enzymic activity and washed thoroughly with buffer. The cell walls were then dried in a graduated acetone series (50, 70, 80, 90, 100%).

4.3. FTIR microscopy

Infrared microscopy of longitudinal thin sections of xylem and interfascicular tissue was carried out as described by Chen et al. (1997) but with vapour phase deuteration (Tsuboi, 1957) in a through-flow hydration cell. A stream of nitrogen was passed through either a drying tube filled with phosphorus pentoxide or a bubbling tube filled with D_2O. The nitrogen line was arranged to allow switching, without exposure to the air, between the drying and deuteration modules. To obtain adequate signal/noise and freedom from diffraction effects each spectrum was recorded from a microscope field of about 1000 μm^2, and the sections were 2–3 cell layers in thickness. Band assignments are based on published data (Sugiyama et al., 1991; Chen et al., 1997; Jarvis and McCann, 2000).

4.4. NMR spectroscopy

Cross-polarisation magic angle spinning (CPMAS) ^{13}C NMR spectra were recorded as described by Newman and Hemmingson (1990), except that the proton spin-lock field remained constant during both CP and data acquisition. The Hartmann-Hahn matching condition was optimised by reducing the ^{13}C field so that signal intensity was maximised (Ha et al., 1997). Resonance assignments are based on published data (Jarvis, 1990; Newman et al., 1996; Ha et al., 1998; Larsson et al., 1997). The principles of the proton spin relaxation editing (PSRE) procedure, used to separate spectral components corresponding to the mobile and rigid domains of the sample, are described in Newman and Hemmingson (1990). The procedure starts from the approximation that the CPMAS spectrum contains two components, the 'mobile' and 'rigid subspectra' S_m and S_r. These were separated by exploiting differences in proton rotating-frame relaxation time constants $T_{1\rho}$ (Newman and Hemmingson, 1995). Briefly, a delay with proton spin-locking is introduced into the pulse sequence immediately before the CP step. During the delay the observed spectrum S_o decays by the $T_{1\rho}$ process to S_g, but the decay is faster for S_m than S_r because these two spectral components differ in proton $T_{1\rho}$. The decay factors for S_m and S_r are denoted by $1/w$ and $1/z$, respectively and are calculated from spectral regions where it can be assumed that only one subspectrum contributes to the signal. Thus, w is calculated from the decay of the signal integrated over the range 53.0–54.5 ppm, which is specific for methoxyl groups assumed to be absent from the rigid component. Similarly z is calculated from the decay of the signal integrated over the range at 83.5–90.0 ppm, specific for C-4 of cellulose which is assumed to be absent from the mobile component. The rigid subspectrum S_r can then be calculated essentially as described by Newman and Hemmingson (1995), although with differences in notation:

$$S_r = \frac{z}{w - z}\left(wS_g - S_o\right)$$

Then $S_m = S_o - S_r$.

The lignin content of the cell walls was determined from their ^{13}C NMR spectrum as follows. The spectral integral in the range 54–58 ppm was used as a measure of the methoxyl content of the lignin, and was ratioed against the integrated intensity of the entire spectrum. The 54–58 ppm spectral region was assumed to contain signals from 15% of the carbon atoms in the lignin macromolecule, on the basis that guaiacyl (G) residues contain one methoxyl carbon atom out of 10 while syringyl (S) residues contain two methoxyl carbon atoms out of 11. Lignin contents calculated in this way are therefore sensitive to variation in the G/S ratio of the lignin. Initially expressed as mol% total carbon in the cell walls, they were corrected to a mass basis on the assumption that the carbon contents of lignin and carbohydrate are 540 and 440 g kg^{-1}, respectively.

Samples were packed in a cylindrical 7 mm diameter Kel-F rotor with fluorocarbon end caps and spun at 3280 Hz. NMR spectra were recorded on a Varian Unity Plus spectrometer at 75.430 MHz for ^{13}C. Parameters of the pulse sequence were: contact time was 0.2 ms; data acquisition time 14.9 ms; recovery delay 2 s. The spectra were derived from 2496 and 10 000 transients for the wild type and *irx3* respectively. The accumulated data were multiplied by Gaussian apodization function with time constant 10 ms before Fourier transformation.

4.5. Chemical analysis of sclerenchyma cell walls

Non-cellulosic polysaccharide components were measured after hydrolysis and conversion to alditol acetates for gas–liquid chromatography (Turner and Somerville, 1997). Cellulose was measured by the Updegraff (1969) method.

Acknowledgements

This work was financially supported by BBSRC, the Royal Society, the EC and EPSRC.

References

Arioli, T., Peng, L., Betzner, A.S., Burn, J., Wittke, W., Herth, W., Camilleri, C., Hofte, H., Plazinski, J., Birch, R., Cork, A., Glover, J., Redmond, J., Williamson, R.E., 1998. Molecular analysis of cellulose synthesis in *Arabidopsis*. Science 279, 717–720.

Chen, L.M., Wilson, R.H., McCann, M.C., 1997. Investigation of macromolecular orientation in dry and hydrated walls of single onion epidermal cells by FTIR microspectroscopy. J. Mol. Struct. 408, 257–260.

Delmer, D., 1999. Cellulose biosynthesis: exciting times for a difficult field of study. Ann. Rev. Plant Physiol. Plant Mol. Biol. 50, 245–276.

Engels, F.M., Jung, H.G., 1998. Alfalfa stem tissues: cell-wall development and lignification. Ann. Bot. 82, 561–568.

Fagard, M., Desnos, T., Desprez, T., Goubet, F., Refregier, G., Mouille, G., McCann, M., Rayon, C., Vernhettes, S., Hofte, H., 2000a. *PROCUSTE1* encodes a cellulose synthase required for normal cell elongation specifically in roots and dark-grown hypocotyls of Arabidopsis. Plant Cell 12, 2409–2423.

Fagard, M., Hofte, H., Vernhettes, S., 2000b. Cell wall mutants. Plant Physiol. Biochem. 38, 15–25.

Goldberg, R., Morvan, C., Jauneau, A., Jarvis, M.C., 1996. Methyl-esterification, de-esterification and gelation of pectins in the primary cell wall. In: Visser, J., Voragen, A.G.J. (Eds.), Pectins and Pectinases. Elsevier Science, Amsterdam, pp. 151–172.

Ha, M.A., Apperley, D.C., Evans, B.W., Huxham, I.M., Jardine, W.G., Viëtor, R.J., Reis, D., Vian, B., Jarvis, M.C., 1998. Fine structure in cellulose microfibrils: NMR evidence from onion and quince. Plant J. 16, 183–190.

Ha, M.A., Apperley, D.C., Jarvis, M.C., 1997. Molecular rigidity in dry and hydrated onion cell walls. Plant Physiol. 115, 593–598.

Helm, R.F., 2000. Lignin-polysaccharide interactions in woody plants. ACS Symp. Ser. 742, 161–171.

His, I., Driouich, A., Nicol, F., Jauneau, A., Hofte, H., 2001. Altered pectin composition in primary cell walls of *korrigan*, a dwarf mutant of *Arabidopsis* deficient in a membrane-bound *endo*-1,4-beta-glucanase. Planta 212, 348–358.

Jarvis, M.C., 1990. Solid-state ^{13}C-n.m.r. spectra of *Vigna* primary cell walls and their polysaccharide components. Carbohydr. Res. 201, 327–333.

Jarvis, M.C., McCann, M.C., 2000. Cell wall biophysics: concepts and methodology. Plant Biochem. Physiol. 38, 1–13.

Lane, D.R., Wiedermeier, A., Peng, L., Hofte, H., Vernhettes, S., Desprez, T., Hocart, C.H., Birch, R.J., Baskin, T.I., Burn, J.E., Arioli, T., Betzner, A.S., Williamson, R.E., 2001. Temperature-sensitive alleles of RSW2 link the KORRIGAN endo-1,4-β-glucanase to cellulose synthesis and cytokinesis in *Arabidopsis*. Plant Physiol. 126, 278–288.

Larsson, P.T., Wickholm, K., Iversen, T., 1997. A CP/MAS C-13 NMR investigation of molecular ordering in celluloses. Carbohydr. Res. 302, 19–25.

Newman, R.H., 1998. Evidence for assignment of ^{13}C NMR signals to cellulose crystallite surfaces in wood, pulp and isolated celluloses. Holzforschung 52, 157–159.

Newman, R.H., Davies, L.M., Harris, P.J., 1996. Solid-state C-13 nuclear magnetic resonance characterization of cellulose in the cell walls of *Arabidopsis thaliana* leaves. Plant Physiol. 111, 475–485.

Newman, R.H., Hemmingson, J.A., 1990. Determination of the degree of cellulose crystallinity in wood by carbon-13 nuclear magnetic resonance spectroscopy. Holzforschung 44, 351–355.

Newman, R.H., Hemmingson, J.A., 1995. Carbon-13 NMR distinction between categories of order and disorder in cellulose. Cellulose 2, 95–109.

Nicol, N., His, I., Jauneau, A., Vernhettes, S., Canut, H., Hofte, H., 1998. A plasma membrane-bound putative *endo*-1,4-β-D-glucanase is required for normal wall assembly and cell elongation in *Arabidopsis*. EMBO J. 17, 5563–5576.

Pear, J.R., Kawagoe, Y., Schreckengost, W.E., Delmer, D.P., Stalker, D.M., 1996. Higher plants contain homologs of the bacterial celA genes encoding the catalytic subunit of cellulose synthase. Proc. Nat. Acad. Sci. USA 93, 12637–12642.

Peng, L.C., Hocart, C.H., Redmond, J.W., Williamson, R.E., 2000. Fractionation of carbohydrates in *Arabidopsis* root cell walls shows that three radial swelling loci are specifically involved in cellulose production. Planta 211, 406–414.

Peng, L.C., Xiang, F., Roberts, E., Kawagoe, Y., Greve, L.C., Kreuz, K., Delmer, D.P., 2001. The experimental herbicide CGA 325′ 615 inhibits synthesis of crystalline cellulose and causes accumulation of non-crystalline β-1,4-glucan associated with CesA protein. Plant Physiol. 126, 981–992.

Sato, S., Kato, T., Kakegawa, K., Ishii, T., Liu, Y.-G., Awano, T., Takabe, K., Nishiyama, Y., Kuga, S., Sato, S., Nakamura, Y., Tabata, S., Shibata, D., 2001. The role of the putative membrane-bound *endo*-1,4-β-glucanase KORRIGAN in cell elongation and cellulose synthesis in *Arabidopsis thaliana*. Plant Cell Physiol. 42, 251–263.

Shedletzky, E., Shmuel, M., Delmer, D.P., Lamport, D.T.A., 1990. Adaptation and growth of tomato cells on the herbicide 2,6-dichorobenzonitrile leads to production of unique cell-walls virtually lacking a cellulose-xyloglucan network. Plant Physiol. 94, 980–987.

Sugiyama, J.J., Persson, J., Chanzy, H., 1991. Combined infrared and electron-diffraction study of the polymorphism of native celluloses. Macromolecules 24, 2461–2466.

Taylor, J.G., Owen, T.P., Koonce, L.T., Haigler, C.H., 1992. Dispersed lignin in tracheary elements treated with cellulose synthesis inhibitors provides evidence that molecules of the secondary cell-wall mediate wall patterning. Plant J. 2, 959–970.

Taylor, N.G., Laurie, S., Turner, S.R., 2000. Multiple cellulose synthase catalytic subunits are required for cellulose synthesis in *Arabidopsis*. Plant Cell 12, 2529–2539.

Taylor, N.G., Scheible, W.R., Cutler, S., Somerville, C.R., Turner, S.R., 1999. The irregular xylem3 locus of *Arabidopsis* encodes a cellulose synthase required for secondary cell wall synthesis. Plant Cell 11, 769–779.

Tsuboi, M., 1957. Infrared spectrum and crystal structure of cellulose. J. Polym. Sci. 35, 159–171.

Turner, S.R., Somerville, C.R., 1997. Collapsed xylem phenotype of Arabidopsis identifies mutants deficient in cellulose deposition in the secondary cell wall. Plant Cell 9, 689–701.

Updegraff, D.M., 1969. Semimicro detemination of cellulose in biological materials. Anal. Biochem. 32, 420–424.

Wilson, W.D., Barwick, J.M., Lomax, J.A., Jarvis, M.C., Duncan, H.J., 1988. Lignified and non-lignified cell walls from kale. Plant Sci. 57, 83–90.

Zuo, J., Niu, Q.-W., Nishizawa, N., Wu, Y., Kost, B., Chua, N.-H., 2000. *KORRIGAN*, an *Arabidopsis* endoglucanase, localizes to the cell plate by polarized targetting and is essential for cytokinesis. Plant Cell 12, 1137–1152.